-RESEARCH PAPER-

International Journal of Mining and Geo-Engineering

IJMGE

IJMGE 60-1 (2026) 83-90

DOI: 10.22059/IJMGE.2026.380823.595187

Permeability of carbonate rocks of the Chandragiri limestone using discontinuity analysis and rock mass classification system, central Nepal

Kritika Thapa [a, *] and Naresh Kazi Tamrakar [a]

[a] *Central Department of Geology, Tribhuvan University, Nepal.*

Article History:

Received: 13 August 2024.

Revised: 02 November 2025.

Accepted: 02 March 2026.

ABSTRACT

The purpose of this study was to understand rock mass characteristics of carbonate rocks using parameters of RMR and GSI and their bearing on effective porosity or permeability of rocks, which is the crucial entity in the flow and storage of water within a rock mass, which is an important consideration in groundwater investigations. Discontinuity analysis is a technique that describes the geometry and characteristics of joints and fractures in a mass of rock. The carbonate rocks of the Chandragiri Limestone of the Phulchauki Group were assessed for strength, joint volume, spacing, joint conditions, and groundwater. Many researchers use the combined condition value of the Lugeon and the RQD value to develop the empirical relation to estimating them. The maximum RMR (77.50%) and the lowest RMR (51.75%) indicate good to fair rock mass. GSI computed based on structural rating and surface condition rating falls between 33 and 55, indicating a blocky, disturbed structure with a fair to very good surface. GSI* computed using the joint condition and RQD (using empirical equation) falls between 42.53 and 73.85, showing somewhat different results. The rock mass permeability (from RQD) varies from 2 to 8.78, indicating a range from slightly permeable to permeable. The RMR-GSI charts were used to evaluate the permeability of the rock mass, which also indicates slightly permeable to permeable rock mass. The permeability (Lugeon) is more than 100 for all locations classified as very high, indicating the rock is permeable.

Keywords: *Carbonate rocks, Discontinuity analysis, Permeability, Rock mass classification.*

1. Introduction

Groundwater, natural resources, etc., are stored in large quantities in carbonate rocks, which are good for storing and transmitting water, as they are good aquifers [1]. Interconnected fracture and their apertures have primary importance in understanding permeability and groundwater yield [2]. In hard rock formations, the movement of groundwater is typically influenced by cracks, joints, geological boundaries, areas of rock movement, faults, voids, and other discontinuities [3]. The groundwater in hard rocks flows through the permeability of the rock [4]. The rock or soil's intrinsic permeability indicates how well it can transmit fluid when the fluid is in motion in a porous medium [5]. Based on various geological and engineering parameters, RMR provides information about the overall strength of rock masses [6] and GSI provides a rock mass's overall quality and intactness [7]. Intact rock mass properties and discontinuities govern the rock mass characteristics [8]. Sonmez and Ulusay [9, 10] analyzed the GIS method of previous authors and modified the GSI to provide a more quantitative basis for evaluating GSI values. Intact or massive rocks are mainly impermeable and the rock masses having discontinuities can be permeable. It provides the pathways which lead to the flow of water which may impact the permeability of rock mass [11]. Somodi et al. [12] emphasize the importance of understanding rock mass properties by describing relationships between GSI chart ratings and GSI values based on RMR.

However, direct measurement of the rock mass permeability is challenging without performing tests. Kayabasi et al. [13] determine Rock quality designation (RQD), weathering degree, discontinuity roughness, and discontinuity fillings of core runs from drillings along with Lugeon tests and derive an empirical relation. RQD, GSI, and Lugeon values were combined to generate a relation among them [14]. Lugeon [15] introduced a technique known as the Lugeon test, used for assessing the transmissivity of a rock mass that involves pressurizing water in a borehole in a rock mass and monitoring the water loss over a specific period. The objective of this research was to characterize rock masses of the Chandragiri Limestone by analyzing discontinuity and rock mass rating parameters and estimating permeability using empirical relations. It provides useful insights into how rock discontinuity parameters can be used to estimate permeability, contributing to a better understanding of groundwater flow in the region. How do discontinuities and rock mass characteristics (assessed by RMR and GSI), influence the permeability of the Chandragiri Limestone? By addressing this question, the research tries to find a condition of Groundwater, with broader implications for its management in carbonate rock formations.

2. Geological setting of the area

The Himalayan orogeny caused extensive bending and faulting in the Kathmandu Valley's rocks. Its center is covered by Quaternary lacustrine deposits, whereas its surroundings are formed by the Lesser Himalayan sedimentary, meta-sedimentary, and metamorphic rocks [16]. The Lesser Himalayas rocks are divided into the Kathmandu Complex and the Nawakot Complex [16, 17]. The Kathmandu Complex is divided into

* Corresponding author. *E-mail address:* thapakritika54@gmail.com (K. Thapa).

the Bhimphedi Group and the Phulchauki Group. The Chandragiri Limestone of the Paleozoic age is the prominent formation of the Phulchauki Group.

The Chandragiri Limestone is underlain by the Sopyang Formation and overlain by the Chitlang Formation. The Chandragiri Limestone contains blue-grey fine-grained siliceous and dolomitic limestone [16] and is well-exposed around the southern and northern areas.

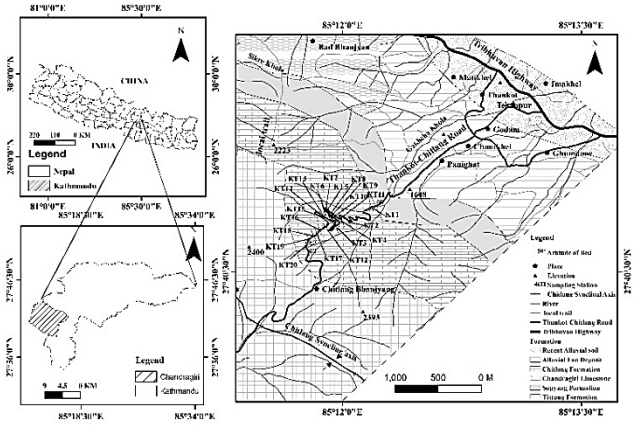

Fig. 1. Location map of the Study area.

In the southern part, it rests over the Sopyang Formation and gives way to the Chitlang Formation with transitional contacts, and it also forms a limb of the syncline, the core of which lies at the summit of the Chandragiri Range. In the Chandragiri Limestone, the rocks are slightly moderately weathered, ranging from thin to massive bedded. The lower part consists of bluish to greyish fine crystalline limestone with phyllite parting and metasandstone interbedded, whereas the middle and upper parts comprise siliceous limestone. The small-scale folds are also visible in the middle portion. Moving towards the Chandragiri Range along the road section, the white to pink quartzite of the Chitlang Formation indicates the contact between the Chandragiri Limestone and the Chitlang Formation.

3. Methodology

After the preliminary study, detailed fieldwork was conducted. Twenty sampling locations were selected, considering geological representativeness and avoidance of repeated strata to ensure uniformity. Each site was chosen based on its distinct structural characteristics, ensuring a diverse and reliable dataset. Information on lithology, geological structures, rock types, and discontinuities was collected carefully.

3.1. Discontinuity analysis:

The orientation of discontinuities, including joints, fractures, and bedding planes, was measured using a geological compass. Spacing between discontinuities was measured using a measuring tape. Persistence, Aperture sizes, infilling material, weathering condition, and surface roughness of discontinuities were qualitatively assessed using visual inspections and compared against standard criteria. The value for each discontinuity set was assigned following Bieniaswki's [6] table guidelines to standardize observations across all sampling locations. The data obtained were used for evaluations of both GSI and RMR.

3.2. Rock Mass Ratings (RMR)

Five parameters were determined to assess the RMR based on Bieniawski's [6] table. Five parameters are discussed below:

Uniaxial Compressive Strength (UCS):

Uniaxial Compressive Strength (UCS) was estimated in the field using a geological hammer and hand nails following the criteria set by Brown [18]. The value obtained was then compared with the Bieniaswki [6] table.

Rock Quality Designation (RQD):

Rock Quality Designation (RQD) was calculated using Palmstrom's [19] equation;

$$RQD=115-3.3Jv \quad (i)$$

where Jv represents the volumetric joint count. The following equation was used:

$$Jv=1/S1+1/S2+.....+1/Sn \quad (ii)$$

where, S1, S2, ... Sn are the average in spacing in meters for the joint sets, and n represents the random joint set available in the sampling area.

Spacing of discontinuities:

The minimum and maximum spacing for each joint set present in the sampling location was measured using a measuring tape. The average spacing of each joint set was calculated and ratings were given based on the Bieniawski [6] table. Then the ratings of every joint set were averaged and the final rating of spacing was obtained.

Joint condition:

Parameters such as joint persistence, aperture, surface roughness, infilling materials, and weathering grade were qualitatively evaluated based on visual assessments and a rating was given according to Bieniawski's [6] table. Then, the rating for each parameter joint set was averaged. The obtained average of each parameter was summed and the final rating of the joint condition was obtained.

Groundwater condition:

Observations related to groundwater presence were made during field visits. The ratings were assigned based on site conditions as given by Bieniawski's [6] classification system.

After rating all five individual parameters, it was added and the final RMR value was obtained.

3.3. Geological Strength Index (GSI):

The Geological Strength Index was calculated using two different methods.

3.3.1. Based on Structural rating (SR) and Surface condition Ratings (SCR)

Sonmez and Ulusay [10], modified the existing GSI chart and introduced two key parameters: Structural Rating (SR) and Surface Condition Rating (SCR). The SR was derived from the volumetric joint count (Jv) using the equation:

$$SR=-17.5\ln(Jv)+79.8 \quad (iii)$$

SCR was calculated based on the surface condition of discontinuities, including roughness, weathering, and infilling materials, as:

$$SCR=a+b+c..... \quad (iv)$$

where, a, b, and c represent the ratings for roughness, weathering, and infilling, respectively. The GSI value was obtained by plotting SR and SCR on the quantitative GSI chart against each other.

3.3.2. Based on joint condition and rock quality designation

In Hoek et al. [20] approach, two parameters of Rock mass Ratings, Rock Quality Designation (RQD) and Joint condition (Jcond89) were used. The Geological Strength Index (GSI*) in this method was calculated as:

$$GSI^*=1.5\,(Jcond89)+0.5\times RQD.... \quad .(v)$$

3.4. Permeability

Direct testing of permeability was not feasible in this study. So, three different empirical methods were used to estimate the permeability. The empirical methods, containing parameters of RMR and the GSI, were chosen for their reliability and relevance.

3.4.1. Based on RQD

Kayabasi et al. [13] used the dataset of 453 cases with the Lugeon test value, along with corresponding RQD, Spacing of Discontinuity, and SCR properties. The dataset was from various dams and coal mines having different lithologies (such as Granite, diorite, volcanic breccia, andesite, and agglomerate). They used these datasets to develop ANFIS (Adaptive Neuro-Fuzzy Inference System) and multiple regression models to derive an empirical relationship for the calculation of rock mass permeability. They also performed simple regression analysis for rock mass permeability with RQD, Spacing of Discontinuity, and SCR using linear, exponential, power, and logarithmic functions. They used the obtained highest coefficient of correlation to estimate rock mass permeability. The simple regression analysis indicates that RQD shows a positive relationship and is statistically useful in estimating rock mass permeability values, while the spacing of discontinuity and SCR is less significant. Although they utilized both ANFIS and non-linear multiple regression models based on various discontinuity parameters But, in this study, only a non-linear simple regression equation based on RQD was used to estimate the rock mass permeability. The equation is as following:

$$\text{Rock mass permeability} = -8.665 \ln(\text{RQD}) + 41.229 \quad \text{..... (vi)}$$

Although RQD is an important parameter to estimate the permeability sometimes it is not enough. In some situations, other parameters also show both positive and negative relationships with rock mass permeability due to the behavior of the material.

3.4.2. Based on the Rock mass permeability (RMP)-Geological strength index (GSI) chart

The RMP-GSI chart was developed by Kayabasi [11] using 365 lugeon test data along with corresponding Rock Quality Designation (RQD), weathering degree, discontinuity roughness, and discontinuity fillings of core runs. The surface condition ratings (SCR) and structure rating values (SR) were defined to determine the GSI values. The Lugeon value and GSI value have coincided with the quantitative GSI chart. The quantitative GSI chart was separated with corresponding permeability values, and a chart was prepared. This chart was utilized to estimate the permeability of carbonate rocks in the Chandragiri Limestone. The quantitative GSI chart, where SR and SCR value was plotted, coincided with the RMP-GSI chart, and the permeability was obtained.

Although the RMP-GSI chart was applied to estimate permeability in this study, this chart was developed primarily for non-soluble rock types because the application to carbonate rock masses with potential karstic features or soluble characteristics may hamper data accuracy. However, the Chandragiri Limestone in this study does not exhibit visible karstic features or cavities.

3.4.3. Based on the joint condition and rock quality designation

Öge [14] established relationships among rock mass classification parameters (GSI and RQD) and permeability (Lugeon). He has tested and evaluated a variety of rock types and discontinuity conditions and provided equations. He correlated GSI, RQD, and Lugeon values. The best-fitted line was drawn, and an equation was obtained. Thus, obtained equation was rearranged with the equation given by Hoek et al. [20]. The final equation was obtained. The obtained equation (vii) was used in this study to estimate Rock mass permeability because it consists of pre-existing and commonly used parameters.

$$\text{Permeability of rock mass} = e^{[5.5 + (16.5\text{Jcond}-165) / \text{RQD}] - 1} \quad \text{..... .. (vii)}$$

The equations given for permeability were considered valid for only the GSI < 60 and all RQD values.

4. Result

4.1. Lithological description of sampling station

Twenty sampling sites lie within elevations ranging from 1723 m to 2066 m (Figure 1) and are oriented towards the SW direction, the dip amount ranging from 42-62 degrees towards the south. In some fractured zones and the upper portion of the bedrock, sparse vegetation is present. The outcrop extension is higher in the lower portion followed by the middle and then by the upper portion. Some of the areas near the sampling location are highly jointed and fractured resulting in landslides. Most of the sampling location shows high persistence i.e.>10m. The sampling location KT2 has very low persistence and mostly, it is covered with sparse vegetation. Thin to medium bedded, finely crystalline, fresh to slightly weathered, bluish-grey limestone with very thin phyllite partings indicates the Chandragiri Limestone. The sampling locations are slightly to moderately weathered. The lower and middle parts contain thin to massive beds, whereas the sampling location of the upper part is very thin to thick-bed. The lower portion exhibits bluish-grey, yellowish, and brown, whereas the middle and upper portions are bluish-grey. All sampling locations have finely crystalline grain sizes. The lamination is visible within the exposure of the sampling location of the middle portion e.g. location KT14. The limestone along with dark grey metasandstone is present in the older sequence. The limestone of sampling location KT20 is intercalated with the thin-bedded fine-grained meta-siltstone. The ripple marks are visible in the limestone bed along with the quartz veins. The traces of the pyrite and iron oxide are excessive in some sampling locations. The calcite leaching is common in the upper portion. The calcite crystal fills the secondary pores within the bed of some sampling sites. The white-to-pink laminated quartzite is dominant near the contact between the Chandragiri Limestone and the Chitlang Formation. Exposures near contact of the Chitlang Formation and the Chandragiri Limestone are severely worn and distorted.

4.2. Discontinuity analysis

The Rock mass of the Chandragiri Limestone is oriented towards the SW direction, the dip amount ranging from 42-62 degrees towards the south. The spacing of discontinuity of the rock mass ranges between 60 mm and 2 m. The persistence rating of sampling location KT19 is highest i.e.4.67 and lowest is of KT10. The aperture rating is the highest of KT19 and the lowest of KT5. The joint condition value of sampling location KT18 is the highest and the sampling location KT7 has the lowest value. The overall joint condition of the study area is good. The ratings for the discontinuity can be seen in Table 1.

4.3. Rock Mass ratings (RMR)

On the Thankot-Chitlang road segment, RMR of the 20 exposed surfaces from the Chandragiri Limestone was carried out. Sampling locations KT3, KT5, KT6, KT7, and KT13 have weaker strengths than the remaining sampling locations (Table 1). The RQD values of KT4 were higher compared to other sampling locations. The exposed surface's groundwater conditions were entirely dry. The RMR value varies between 51.75% and 77.5%. In terms of rock mass categorization, the rock masses of the Chandragiri Limestone were classified as fair to good (Table 1). The presence of discontinuities, such as small-scale folds and joint fractures, influences the RMR value because their orientation and spacing influence the stability of rocks. Sampling locations such as KT5, KT6, etc. have higher discontinuities, due to which they have lower RMR values. The discontinuities reduce intact rock by reducing overall rock quality. Another influencing factor could be the weathering of limestone. Weathered sampling locations show lower RMR values than fresh, unaltered sampling locations.

4.4. Geological Strength Index (GSI)

The GSI was used to estimate the strength and deformability of rock masses, which was needed for statistical analysis [21, 22]. Various measures have been developed and modified for the construction of projects such as tunnels, slopes, etc., especially in heterogeneous rock [9, 10, 23, 24]. The GSI was evaluated using two different methods described in the following sections.

Table 1. Rock mass characterization of the rock masses of the Chandragiri Limestone.

SN	Strength (R1)		RQD (R2)		Spacing (R3)								Joint condition (R4)						GW Cond. (R5)	*RMR	Rock Classification	
					J1		J2		J3		J4											
	V (Mpa)	R1	V (%)	R2	V (m)	Ra	V (m)	Rb	V (m)	Rc	V (m)	Rd	*R3	PR	SR	RR	IMR	WC	**R4				
KT1	100-250	12	88.96	17	0.52	10	0.26	10	0.48	10			10	3.33	3.33	5.33	5	2	18.99	15	72.99	II	Good
KT2	100-250	12	64.28	13	0.3	10	0.27	10	0.12	8			9.33	2.67	2	3.67	3.67	2	14.01	15	63.34	II	Good
KT3	100-250	7	56.23	13	0.38	10	0.16	8	0.21	10	0.24	10	9.5	4	2.75	4	3.5	2	16.25	15	60.75	II	Good
KT4	100-250	12	92.53	20	0.7	15	0.34	10	0.41	10			11.66	3.33	1.67	4.33	4.33	1.33	14.99	15	73.65	II	Good
KT5	50-100	7	42.30	8	0.23	10	1	8	0.23	10	0.3	10	9.5	3.25	1.5	2	3.5	4	14.25	15	53.75	III	Fair
KT6	50-100	7	49.07	8	0.18	8	0.13	8	0.33	10	0.27	10	9	3.5	1.75	2.5	3.5	1.5	12.75	15	51.75	III	Fair
KT7	50-100	7	52.33	13	0.48	10	0.12	8	0.37	10	0.17	8	9	3.5	1.5	3	4	1	13	15	57.00	III	Fair
KT8	100-250	12	61.84	17	0.31	10	0.12	8	0.38	10	0.52	10	9.5	2.75	3.5	3.5	5	3	17.75	15	71.25	II	Good
KT9	100-250	12	48.41	8	0.32	10	0.18	8	0.23	10	0.14	8	9	5	4	4	5	4	22	15	66.00	II	Good
KT10	100-250	12	80.61	17	0.44	10	0.6	15	0.2	10	0.65	15	12.5	2.25	4.25	4.5	5	5	21	15	77.50	II	Good
KT11	100-250	12	84.97	17	0.39	10	0.3	10	0.72	15	0.55	10	11.25	1	3.25	3	5	3	15.25	15	70.50	II	Good
KT12	100-250	12	79.16	17	0.57	10	0.21	10	0.23	10			10	3.33	3	3	5	2.67	17	15	71.00	II	Good
KT13	50-100	7	56.92	13	0.26	10	0.23	10	0.18	8	0.26	10	9.5	4	3.75	2.5	5	3	18.25	15	62.75	II	Good
KT14	100-250	12	49.30	8	0.17	8	0.22	10	0.16	8	0.31	10	9	4	3.25	3.5	5	1.5	17.25	15	61.25	II	Good
KT15	100-250	12	63.98	13	0.32	10	0.25	10	0.12	8			9.33	3.33	1.67	3	3	1.33	12.33	15	61.66	II	Good
KT16	100-250	12	87.28	17	0.4	10	0.32	10	0.51	10			10	3.33	1	4.66	3	2	13.99	15	67.99	II	Good
KT17	100-250	12	82.43	17	0.21	10	0.51	10	0.31	10			10	4	2.33	5.33	3.67	2.67	18	15	72.00	II	Good
KT18	100-250	12	50.95	13	0.46	10	0.19	8	0.32	10	.11	8	9	4.5	5	4.75	5	3	22.25	15	71.25	II	Good
KT19	100-250	12	54.54	13	0.3	10	0.14	8	0.12	8			8.67	4.67	4.33	5.33	5	2	21.33	15	70.00	II	Good
KT20	100-250	12	88.68	17	0.39	10	0.32	10	0.43	10			10	4	4	4.67	5	2	19.67	15	73.67	II	Good

*RMR=R1+R2+R3+R4+R5 *R3=Average of (Ra+Rb+Rc+Rd) **R4=PR+SR+RR+IMR+WR

V= Value R= Rating PR=Persistence Rating SR=Separation Rating RR=Roughness Rating IMR=Infilling Material Rating WR=Weathering Rating GW cond.=Groundwater Condition

4.4.1. GSI from SR and SCR

According to Sonmez and Ulusay [10], GSI was evaluated (Table 2). The joint spacing, orientation, etc., were visualized in Structural Rating (SR), and the rock surfaces such as weathered, smooth, and roughness, were evaluated in Block surface condition rating (SCR). The SR provides critical insights into rock mass stability. As the volumetric joint count increases, the SR decreases, indicating that a higher density of joints negatively impacts the rock's structural integrity.

The study area has a blocky disturbed and very blocky rock structure with fair to very good surface condition. (Figure 2) The sampling stations KT1, KT4, KT11, KT16, and KT20 indicate a very blocky rock structure and the remaining sampling locations indicate a blocky disturbed rock structure. The sampling locations KT10 have very good surface conditions.

Sampling locations KT1, KT8, KT9, KT11, KT 17, KT18, KT19, and KT20 have good rock surface conditions and the remaining sampling locations have a fair surface condition with blocky disturbed structure. The highest GSI obtained is 55 of sampling location KT10. SR has quite a higher value than SCR because only the spacing influences the SR, but SCR is influenced by the weathering, roughness, and infilling of rock mass. The sampling locations with higher SR and SCR values have higher GSI values and vice versa. The sampling locations KT1, KT10, etc. have higher SR and SCR possessing higher GSI values whereas the sampling locations KT5, KT6, etc. having lower SR and SCR have lower GSI values than others.

4.4.2. GSI from joint condition data (Jcond89) and RQD*

The GSI* obtained from the equation suggested by Hoek et al. [20] has a higher value than the GSI from Sonmez and Ulusay [10] method. The GSI* has the highest value of sampling location KT20 i.e. 73.85 and the second highest value of location KT1 i.e. 72.97. The lowest value is of sampling location KT5 i.e. 42.53 (Table 2). The discontinuity parameters and the RQD value play an important role in the value of the GSI*. The Sampling location having the highest RQD and joint condition rating has a good GSI* value, and vice versa.

4.5. Correlation between Rock mass rating and Geological strength indices

The data of RMR, GSI, and GSI* were plotted. By establishing a correlation between the RMR and GSI, RMR and GSI*, and GSI and GSI*, we can gain insights into the properties of the intact rock and its discontinuities. The RMR values fall within the range of 51.75% to 77.5%, which classifies the rock type as good to fair. The GSI values vary from 33 to 55. And GSI* ranges from 42.53 to 73.85. Scatter plots illustrating the relationships between RMR and GSI (Fig. 2), RMR and GSI* (Figure 3), and GSI and GSI* (Figure 4) are moderate to strongly positive. When the RMR increases, the GSI and GSI* tend to increase. This relationship demonstrates that greater GSI values are linked to higher RMR values. The distribution of the majority of data points lies around the regression line, showing that most points are close to the regression line, which indicates a positive but not perfect correlation.

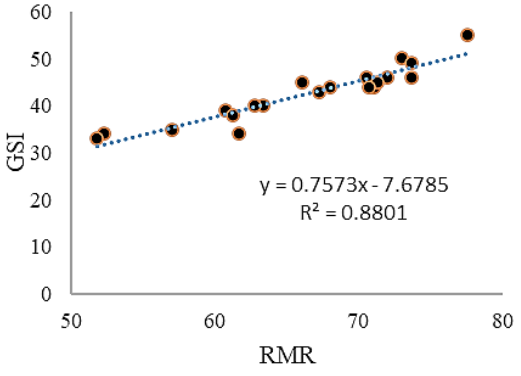

Fig. 2. Correlation between the RMR and GSI.

Table 2. Geological Strength Indices of the sample location of the study area.

S. N	Joint Volume (Jv)	Structure Rating (*SR)	Joint condition ($Jcond_{89}$)				GSI (from SR and SCR)	***GSI* (from J $cond_{89}$ and RQD)
			Roughness ratings (a)	Infilling materials Rating (b)	Weathering Rating (c)	**SCR		
KT1	7.89	43.65	5.33	2	5	12.33	50	72.97
KT2	15.37	31.98	3.67	2	3.67	9.34	40	53.15
KT3	17.81	29.40	4	2	3.5	9.5	39	52.49
KT4	6.81	46.23	4.33	1.33	4.33	9.99	46	68.75
KT5	22.03	25.68	2.5	3.5	3.5	9.5	34	42.53
KT6	19.98	27.39	2.5	1.5	3	7.5	33	43.66
KT7	18.99	28.28	3	1	4	8	35	45.67
KT8	16.11	31.16	3.5	3	5	11.5	43	57.54
KT9	20.18	27.22	4	4	5	13	45	57.20
KT10	10.42	38.78	4.5	5	5	14.5	55	71.81
KT11	9.1	41.16	3	3	5	11	46	65.36
KT12	10.86	38.06	3	2.67	5	10.67	44	65.08
KT13	17.6	29.61	2.5	3	5	10.5	40	55.84
KT14	19.91	27.45	3.5	1.5	5	10	38	50.52
KT15	15.46	31.88	3	1.33	3	7.33	34	50.49
KT16	8.4	42.56	4.66	2	3	9.66	44	64.63
KT17	9.87	39.73	5.33	2.67	3.67	11.67	46	68.21
KT18	19.41	27.90	4.75	3	5	12.75	45	58.85
KT19	18.32	28.91	5.33	2	5	12.33	44	59.27
KT20	7.975	43.46	4.67	2	5	11.67	49	73.85

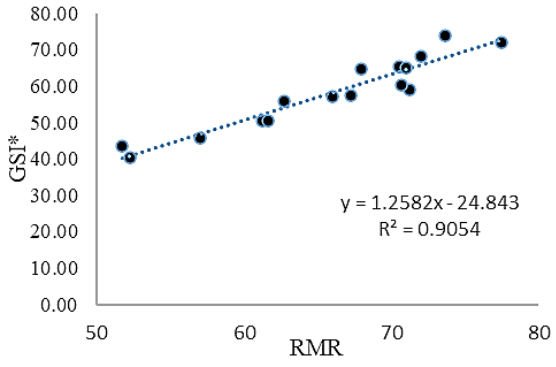

Fig. 3. Correlation between the RMR and GSI*.

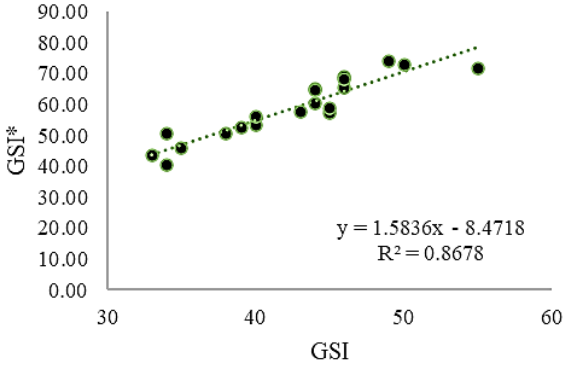

Fig. 4. Correlation between the GSI and GSI*.

4.6. Permeability

Permeability controls the movement of fluids in the subsurface and tells us how well a material can accommodate the passage of gases or liquids like water. RMR gives a broad picture but does not give a precise measurement of permeability. A direct measurement of permeability is not provided by GSI, but it does reflect potential fluid flow through the rock mass indirectly. The geological variability along with other elements like joint spacing, groundwater conditions, infill materials, etc. were considered. When discontinuities exist in rock, the permeability of the rock is controlled not only by the intact rock but also by the discontinuities that separate the intact rock blocks [25]. The persistence, tightness, aperture, roughness, kind of infill, and filling thickness are some of the features of discontinuities that affect a rock mass's strength and water flow rate [14]. The permeability of the rock mass is calculated empirically.

4.6.1. Based on RQD

According to the equation given by Kayabasi et al. [13], the rock mass permeability is calculated (Table 3). The lowest value of permeability is of sampling location KT4 (i.e. 2) indicating slightly permeable rock mass and the highest value is of sampling location KT5 (i.e. 8.78) indicating permeable rock mass. The sampling location having a higher RQD shows a lower value and vice versa. The sampling locations KT1, KT4, KT10, KT11, KT12, KT16, KT17, and KT20 exhibit slightly permeable rock mass whereas the remaining sampling locations have permeable rock mass.

4.6.2 Based on the Rock mass permeability (RMP) - Geological Strength Index (GSI) chart

Kayabasi [11] made some derivations based on the RMP-GSI chart for the rock mass permeability (Figure 6). Rock mass is impermeable or somewhat permeable when its GSI value equals or exceeds 60. It is permeable or very permeable when its GSI value is equal to or less than 20 and for the values between 20 and 60, the RMP-GSI chart should be considered. A decrease in ratings can indicate increased permeability in

Table 3. Rock mass permeability from empirical method.

Location	RQD	Joint condition	RMP [14]	Classification [26]	RMP [11]	Classification [15]
KT1	88.96	18.99	476.93	very high	2.34	Slightly permeable
KT2	64.28	14.01	251.98	very high	5.15	Permeable
KT3	56.23	16.25	563.45	very high	6.31	Permeable
KT4	92.53	14.99	219.17	very high	2.00	Slightly permeable
KT5	42.30	14.25	472.37	very high	8.78	Permeable
KT6	49.07	12.75	226.96	very high	7.49	Permeable
KT7	52.33	13	231.80	very high	6.94	Permeable
KT8	61.84	17.75	711.90	very high	5.49	Permeable
KT9	48.41	22	5379.78	very high	7.61	Permeable
KT10	80.61	21	855.32	very high	3.19	Slightly permeable
KT11	84.97	15.25	249.50	very high	2.74	Slightly permeable
KT12	79.16	17	387.24	very high	3.35	Slightly permeable
KT13	56.92	18.25	983.89	very high	6.21	Permeable
KT14	49.30	17.25	1019.04	very high	7.45	Permeable
KT15	63.98	12.33	164.17	very high	5.19	Permeable
KT16	87.28	13.99	191.39	very high	2.50	Slightly permeable
KT17	82.43	18	446.47	very high	3.00	Slightly permeable
KT18	50.95	22.25	4756.93	very high	7.17	Permeable
KT19	54.54	21.33	2772.26	very high	6.58	Permeable
KT20	88.68	19.67	544.12	very high	2.37	Slightly permeable

rock masses [11]. On coinciding the plotted data (Figure 5) with the RMP-GSI chart (Figure 6) we observed that the value lies in the slightly permeable (around less than 5 Lugeon region) and permeable region (around 5-25 Lugeon region). There is neither intact nor massive nor blocky nor disintegrated rock mass structure. Absence of Poor and very poor surface conditions in the chart indicating neither impermeable nor very permeable rock masses are present. The sampling locations having a good or very good surface condition with a blocky or blocky disturbed structure lie in the region around 1-5 lugeon values indicating a slightly permeable rock mass whereas the sampling location with a blocky disturbed structure and good to fair surface condition lie in the region of 5-25 lugeon value indicates a permeable region. The sampling location KT1, KT4, KT10, KT11, KT12, KT16, KT17, and KT20 lies in the slightly permeable region whereas the remaining stations lie in the permeable region.

4.6.3. Based on a joint condition and RQD

The lowest Lugeon value (uL) is of sampling location KT15 and is followed by location KT16. The value obtained by using the Öge [14] formula lies between 164.17 and 5379.78. (Table 3) According to the table given by Quiñones [26], a lugeon value having less than 1 is classified as very low, 1-5 as low, 5-15 as moderate 15-50 as medium, 50-100 as high, and more than 100 as very high. All the values obtained from this equation are higher than 100. They are classified as very high. It indicates that the rock mass is permeable.

5. Discussions

The investigation of the study area provides insight into rock mass condition and permeability based on it.

5.1. Rock Mass Rating (RMR)

The study exhibits different strengths across sampling locations. Despite having a fine grain and a high proportion of quartz [27] and a fine grain [28]. KT5, KT6, KT7, and KT13 reveal strong strength. The remaining locations are very strong probably due to high joint volume and good weathering conditions. Groundwater conditions do not make any impact. Joint spacing has less influence, but strength and RQD, along with Joint condition have an influential effect on the RMR value.

The sampling locations KT5, KT6, and KT7 having low values of strength, RQD, and Joint condition, have RMR values between 50 and 60. They lie in Class III indicating a “Fair rock” type. All the remaining sampling locations have RMR values ranging between 60 and 80, which lies in Class II indicating a “Good rock” type. The dolomite of the Malekhu Limestone (when performing at two distinctive spots Ml1 and Ml2), the Ml1 has a low value of RQD and Joint condition and Ml2 has a low value of Joint condition along with Damp Groundwater condition resulting in low RMR value i.e. 57 indicating a “Fair rock” type. The dolomite of Dhading Dolomite has a highly jointed and fractured rock mass with very low RQD resulting in an RMR value of 52 [29, 30]. The RMR of the Chandragiri Limestone ranges from 51.75% to 77.5% which overlaps with them at the lower end. The study area has completely dry groundwater conditions and other parameters with high values (mainly RQD and Joint condition) compared to the Malekhu Limestone and the Dhading Dolomites resulting in some higher RMR ratings. While both are classified as “Fair rock,” the Chandragiri Limestone exceeds this classification and is classified as a “good rock” type.

The carbonate rock of the Sabzkuh water conveyance project has very low strength and groundwater condition due to which they have low RMR. The value ranges from 14 to 56 indicating a “very poor to fair rock” type [31]. Their value indicates poor rock mass quality than our study site. All the parameters, strength, RQD, Joint spacing, Joint condition, and Groundwater condition play a crucial role in the better RMR value. A lower rating of any of the parameters restricts to a better rock type. The sampling location KT4 has a good rating for almost all parameters but the rating of joint condition is slightly low restricting the rock to good rock from being a very good rock type. The condition is similar for the three sampling locations of the Limestone rock mass of Gunung Lang, Ipoh, Perak. Despite having good ratings for all the parameters, the strength is low due to which the RMR values are restricted to 77, 77, and 82 [32].

5.2. Geological strength indices

The GSI values calculated from SR and SCR range from 33 to 55. SR is more influential than the SCR. The higher the value of SR the higher will be GSI value. The sampling location KT6 with low SCR and SR values has low GSI. Despite having the highest SR, KT4 does not have the highest GSI due to a slightly lower SCR. The GSI value varies depending on the calculation method used, which results in different

GSI values for the same location which can be seen in this study The GSI* calculated from the RQD and Joint Condition method ranges from 42.53 to 73.85. The sampling location KT20 with a high value of RQD and joint conditions has good GSI.

The dolomite of the Malekhu Limestone having low values of SR and SCR has GSI values of 38 and 40 when performing at two different spots Ml1 and Ml2 respectively. This indicates blocky rock structure and fair surface condition which is lower than the Chandragiri Limestone. Due to the low RQD of Dolomite of the Dhading Dolomite, the method of Osgoui et al. [33] was used, resulting low GSI value i.e.16 [29]. According to Hashemi et al. [31], the GSI value of the carbonate rock of the Sabzkuh water conveyance project which was calculated from overview and structural geology and compared with Hoek and Brown [22] ranges from 22 to 60. This indicates the disintegrated blocky. Those, which were calculated based on the Block volume and joint surface condition factors suggested by Cai et al. [34] range from 25 to 56.

5.3. Correlation between rock mass ratings and geological strength indices

The parameters used for the assessment of both the RMR and GSI are consistent throughout the study. Moderately strong to positive relationship is consistently developed between the RMR-GSI, RMR-GSI*, and GSI-GSI*, with R^2 values of 0.8801, 0.9054, and 0.8678 respectively. The RMR and GSI of the Lesser Himalaya have a good and positive correlation with R^2=0.57 which is less than the Chandragiri Limestone because of distinct lithological characteristics, and structural and geological features that impact the RMR and GSI [29].

5.4. Permeability

The Chandragiri Limestone has quite a high RMR and GSI value. The rock mass having lower RMR and GSI values may be expected to have higher permeability because the higher is expected to have weaker strength and quality. The Rock mass permeability value of limestone of the Chandragiri Limestone calculated by using the regression equation given by Kayabasi et al., [13] ranges from 2 to 8.78. This is consistent with, the value derived from the evaluation of the RMP-GSI chart given by Kayabasi [11] which also shows slightly permeable to permeable rock mass. The rock mass permeability for the same sampling location reveals significant variability due to using of different methods given by different authors. According to the empirically derived formula by Öge [14], the permeability (Lugeon) value has been calculated and classified by using the Quiñones [26]. The value obtained for the carbonate rock of the Chandragiri Limestone by this method is higher than 100 which is classified as very high. It describes the rock mass condition as the open closely spaced voids. The study area is highly permeable [35, 36]. Among the three approaches used for the calculation, two of the approaches given by Kayabasi et al. [13] and Kayabasi [11] exhibit the same result.

The permeability value that was obtained from various discontinuity analyses and rock mass classifications highlights both the potential influence on the stability of the road section and its role in groundwater flow and resource management in the study area. As it lies on the road section, it indicates that their need for a targeted rock mass assessment in road section maintenance, where high permeability may hamper the road stability and safety as well as groundwater management strategies.

6. Conclusions

This study emphasizes discontinuity analysis, rock mass classification, and permeability assessments, which provide essential insights into both geological characteristics and potential engineering applications. The Rock Mass Rating (RMR) ranges from 51.75% to 77.50%, classifying the Chandragiri Limestone as a fair to good rock type. The younger stratigraphic segment has a significantly greater RMR value than the older portions. The GSI* based on two parameters of RMR i.e. RQD and joint condition, ranges from 42.53-73.85 indicating poor to high rock quality. The GSI based on SR and SCR ranges from 33-55, indicating fair to very good rock surface condition with blocky disturbed structure.

The RMR, GSI, and GSI* when correlated with one another exhibit a moderate to strong positive correlation. Joint condition plays a major role in both RMR and GSI's ratings.

The rock mass permeability of the Chandragiri Limestone displays a wide variation from slightly permeable to highly permeable depending on the method used for the calculations. It helps to understand the rock mass. This high permeability indicates the presence of fractures and voids, affecting stability and quality, and impacting both groundwater flow and infrastructure resilience in the area. This inconsistency in permeability value may impact the infrastructure design, construction, maintenance, and road safety. It also makes an implication for understanding and managing groundwater flow.

At last, this study underscores the inevitability of detailed geological assessments for better and more durable road sections and groundwater planning. The methodologies used, help for preliminary investigations and provide a foundation for further studies and practical applications in similar geological environments.

Acknowledgement

The authors are grateful to the Central Department of Geology for providing a laboratory facility.

References

[1]. Dasgupta, T. and Mukherjee, S., 2020. Porosity in Carbonates. In Advances in Oil and Gas Exploration and Production, 9–18. Springer. https://doi.org/10.1007/978-3-030-13442-6_2

[2]. Gudmundsson, A., Fjeldskaar, I. and Gjesdal, O., 2002. Fracture-generated permeability and groundwater yield in Norway. Norges geologi ke undersoke/se Bulletin, 439, 61-69.

[3]. Singhal, B. B. S. and Gupta, R. P., 1999. Applied hydrogeology of fractured rocks. The Netherlands, Kluwer Academic Publ. 401 pp. https://doi.org/10.1007/978-90-481-8799-7

[4]. Gudmundsson, A., Gjesdal, O., Brenner, S. L., and Fjeldskaar, I. 2003. Effects of linking up of discontinuities on fracture growth and groundwater transport. Hydrogeology Journal, 11 (1), 84–99. https://doi.org/10.1007/s10040-002-0238-0

[5]. Schwartz, F.W. and Zhang, H., 2003. Fundamentals of Groundwater. John Wiley & Sons, Inc., New York 583Bieniawski, Z. T., 1989. Engineering rock mass classifications: a complete manual for engineers and geologists in mining, civil, and petroleum engineering. John Wiley & Sons.

[6]. Bieniawski, Z. T., 1989. Engineering rock mass classifications: a complete manual for engineers and geologists in mining, civil, and petroleum engineering. John Wiley & Sons.

[7]. Marinos, P., Marinos, V., and Hoek, E., 2007. Geological Strength Index (GSI). A characterization tool for assessing engineering properties for rock masses. Underground Works under Special Conditions - Proceedings of the Workshop (W1) on Underground Works under Special Conditions. 13-21. https://doi.org/10.1201/noe0415450287.ch2

[8]. Şen, Z. and Sadagah, B. H., 2003. Modified rock mass classification system by continuous rating. Engineering Geology, 67(3-4), 269–280. doi:10.1016/s0013-7952(02)00185-0

[9]. Sonmez, H. and Ulusay, R., 1999. Modification to the Geological Strength Index (GSI) and their Applicability to Stability of Slopes, International Journal of Rock Mechanics and Mining Science, 36, 743-760. http://dx.doi.org/10.1016/S0148-9062(99)00043-1

[10]. Sonmez, H. and Ulusay, R., 2002. A discussion on the Hoek–Brown failure criterion and suggested modification to the

criterion verified by slope stability case studies. Yerbilimleri (Earth Sciences), 26, 77–99, www.yerbilimleri.hacettepe.edu.trS

[11]. Kayabaşi, A. 2017. The Geological Strength Index Chart Assessment for Rock Mass Permeability. Bulletin of the Earth Sciences Application and Research Centre of Hacettepe University, 38 (3), 295-309.

[12]. Somodi G, Bar N, Kovács L, Arrieta M, Török Á, Vásárhelyi B., 2021. Study of Rock Mass Rating (RMR) and Geological Strength Index (GSI) Correlations in Granite, Siltstone, Sandstone and Quartzite Rock Masses. Applied Sciences. 11 (8), 3351 pp. https://doi.org/10.3390/app11083351

[13]. Kayabasi, A., Yesiloglu-Gultekin, N., and Gokceoglu, C. 2015. Use of non-linear prediction tools to assess rock mass permeability using various discontinuity parameters. Engineering Geology, 185, 1–9. https://doi.org/10.1016/j.enggeo.2014.12.007

[14]. Öge, I.F., 2017. Assessing Rock Mass Permeability Using Discontinuity Properties, Procedia Engineering. 191, 638 – 645

[15]. Lugeon, M., 1933. Barrages et géologie. Library de l' Université, Paris, Dunod. 430pp.

[16]. Stöcklin, J., 1980. Geology of Nepal and its regional frame. Journal of Geology Society, London, 137, 1-34. http://dx.doi.org/10.1144/gsjgs.137.1.0001

[17]. Stöcklin, J., Bhattarai, K.D., 1977. Geology of the Kathmandu area and central Mahabharat range, Nepal Himalaya. Report of Department of Mines and Geology/ UNDP (unpublished), 86p. http://dx.doi.org/10.1144/gsjgs.137.1.000

[18]. Brown, E.T., 1981. Rock characterization, testing, and monitoring, ISRM suggested methods. Pergamon, Oxford, 171–183.

[19]. Palmstrom A., 1974. Characterization of jointing density and the quality of rock masses (in Norwegian). Internal report, A.B. Berdal, Norway, 26 pp.

[20]. Hoek, E., Carter, T. G., and Diederichs, M.S., 2013. Quantification of the Geological Strength Index Chart. 47th US Rock Mechanics/Geomechanics Symposium, 3, 1757-1764.

[21]. Hoek, E., 1994. Strength of rock and rock masses. News J ISRM, v. 2(2) pp. 4–16Hoek, E., Brown E.T., 1997 Practical estimates of rock mass strength. Int J Rock Mech Min Sci 34(8) 1165–1186

[22]. Hoek, E., Brown E.T., 1997 Practical estimates of rock mass strength. Int J Rock Mech Min Sci 34(8) 1165–1186

[23]. Hoek, E., Marinos, P. G., Benissi, M., 1998. Applicability of the geological strength index (GSI) classification for weak and sheared rock masses—the case of the Athens schist formation. Bull Eng Geol Env, 57(2), 151–160.

[24]. Marinos, P., and Hoek, E., 2000. GSI: a geologically friendly tool for rock mass strength estimation. In: Proceeding of the GeoEng 2000. The International Conference on Geotechnical and Geological Engineering, Melbourne, Technomic publishers, Lancaster, 1422–1446.

[25]. Zhang, L., 2013. Aspects of rock permeability. Frontiers of Structural and Civil Engineering, 7(2), 102–116. doi:10.1007/s11709-013-0201-2

[26]. Quiñones-Rozo, C., 2010. Lugeon test interpretation, revisited, in Collaborative Management of Integrated Watersheds, US Society of Dams, 30th Annual Conference, 405–414.

[27]. Chimouriya, R., 2023. Study on the relationship between slake durability index and point load strength index of limestone from Chandragiri Limestone, Thankot-Chandragiri area, Central Nepal. Master thesis submitted to CDG, Unpublished 85pp

[28]. Yusof, N. Q. A. M., and Zabidi, H., 2016. Correlation of mineralogical and textural characteristics with engineering properties of granitic rock from Hulu Langat, Selangor. Procedia Chemistry, 19, 975-980.

[29]. Singh, J.L. and Tamrakar, N.K., 2013. Rock mass rating and geological strength index of rock masses of Thopal-Malekhu river areas, Central Nepal lesser Himalaya. Bull. Dept. Geol., 16, 29–42.

[30]. Bista, K., and Tamrakar, N. K., 2015. Evaluation of strength and durability of rocks from Malekhu-Thopal Khola area, Central Nepal Lesser Himalaya for construction aggregates. Bulletin of the Department of Geology, 18, 15-34.

[31]. Hashemi, M., Moghaddas, S., & Ajalloeian, R., 2010. Application of rock mass characterization for determining the mechanical properties of rock mass: A comparative study. Rock Mechanics and Rock Engineering, 43(3), 305–320. https://doi.org/10.1007/s00603-009-0048-y

[32]. Lai, T.G., Razib, A.M.M., Mazlan, N.A., Ghani Rafek, A., Serasa, N.A.S., and Mohamed, T.R., 2016. Rock Slope Stability Assessment Using Slope Mass Rating (SMR) Method: Gunung Lang Ipoh Malaysia. Scholars Journal of Engineering and Technology, 4(SJET), 185–192. www.saspublisher.com

[33]. Osgoui, R.R., Ulusay, R. and Unal, E., 2010. An assistant tool for the Geological Strength Index to better characterize poor and very poor rock masses, International Journal of Rock Mechanics and Mining Science, 47, 690-697. http://dx.doi.org/10.1016/j.ijrmms.2010.04.001

[34]. Cai, M., Kaiser, P.K., Uno, H., Tasaka, Y., and Minami, M., 2004. Estimation of rock mass deformation modulus and strength of jointed hard rock masses using the GSI method. Inter J Rock Mech Min Sci, 41, 3–19

[35]. Terzaghi, K., and Peck, R., 1967. Soil Mechanics in Engineering Practice. John Wiley and Sons Inc., New York, 729pp.

[36]. ISRM (International Society for Rock Mechanics), 1981. In: Brown ET, editor. The International Society of Rock Mechanics suggested a method: rock characterization, testing, and monitoring. London: Pergamon Press.